Observation of Gyromagnetic Spin Wave Resonance in NiFe Films

Yuki Kurimune,[1] Mamoru Matsuo,[2,3,4,5] and Yukio Nozaki[1,6]
[1]Department of Physics, Keio University, Yokohama 223-8522, Japan
[2]Kavli Institute for Theoretical Sciences, University of Chinese Academy of Sciences, No. 3, Nanyitiao, Zhongguancun, Haidian District, Beijing 110190, China
[3]CAS Center for Excellence in Topological Quantum Computation, University of Chinese Academy of Sciences, Beijing 100190, China
[4]RIKEN Center for Emergent Matter Science, Wako, Saitama 351-0198, Japan
[5]Advanced Science Research Center, Japan Atomic Energy Agency, Tokai, 319-1195, Japan
[6]Center for Spintronics Research Network, Keio University, Yokohama 223-8522, Japan

(Received 14 January 2020; accepted 5 May 2020; published 27 May 2020)

This Letter demonstrates spin wave resonance (SWR) owing to the gyromagnetic effect by propagating a Rayleigh-type surface acoustic wave (R-SAW) through ferromagnetic thin films. The SWR amplitude in a NiFe film shows a higher-order frequency variation than in a magnetoelastic Ni film. This frequency dependence is well understood in terms of the presence of a gyromagnetic field attributable to the local lattice rotation in the R-SAW. From the frequency dependence of the SWR amplitude, the gyromagnetic SWR could be separated from another SWR caused by a magnetoelastic effect of the ferromagnet.

DOI: 10.1103/PhysRevLett.124.217205

The gyromagnetic effect, which enables a mutual conversion of angular momentum between the mechanical rotation of a ferromagnetic body and its macroscopic magnetic moment, was experimentally demonstrated by Barnett [1,2] and Einstein and de Haas a hundred years ago [3]. The effect is based upon the universal conservation law of angular momentum, because the magnetic moment in a ferromagnetic body arises from a sum of the angular momenta of electrons confined within the body. The fundamental coupling between spin and mechanical rotation is known as the spin-vorticity coupling [4–8] and is given by

$$H_{\mathrm{svc}} = -\frac{\hbar}{4}\boldsymbol{\sigma}\cdot\boldsymbol{\Omega}, \tag{1}$$

where $\boldsymbol{\sigma}$ is the Pauli matrix and $\boldsymbol{\Omega}$ is the vorticity defined by $\boldsymbol{\Omega} = \nabla \times (\partial \mathbf{u}/\partial t)$ with the displacement vector of the lattice $\mathbf{u}$. By analogy with the Zeeman effect, the spin-vorticity coupling is interpreted as a Zeeman coupling due to the effective magnetic field $\boldsymbol{\Omega}/(2\gamma)$, where γ is the gyromagnetic ratio of an electron. The magnetic field is hereafter referred to as the Barnett field. Therefore, the gyromagnetic effect can be enhanced by increasing the rotational frequency. The Barnett field has recently been detected in various materials using nuclear-magnetic [9–11], paramagnetic [12], and ferrimagnetic [13,14] resonances with a rigid rotation at a frequency of 10 kHz. Moreover, spin-current generation in liquid [15] and solid [16,17] metals was observed, where a local rotation, i.e., a vorticity, couples with spin angular momentum via spin-vorticity coupling [18–20]. Recently, it has been demonstrated that a Rayleigh-type surface acoustic wave (R-SAW) could be used to excite a spin wave resonance (SWR) in magnetoelastic Ni films [21,22] over long distances [23] with low power [24]. The lattice deformation in the R-SAW consists of elliptical particle motions in a normal plane parallel to its propagation direction and is characterized by the strain-tensor components of ε_{xx} and ε_{xy}. The equivalent magnetic field of the magnetoelastic (ME) effect is typically given as a product of the strain tensor and the ME-coupling constant of a Ni film. It has been demonstrated experimentally that the existence of an ε_{xy} component leads to a nonreciprocal-SWR excitation [25,26]. These results clearly show that ε_{xx} and ε_{xy} coexist in the R-SAW, which is injected into the metallic thin film deposited on a piezoelectric substrate.

In this Letter, we demonstrate a SWR excitation in a single NiFe thin film by propagating a gigahertz SAW through it. Unlike the SWR excitation using the ME effect in a Ni film, a torque on magnetization is generated by the Barnett field, which is attributed to Ω in the NiFe film. In order to distinguish the Barnett effect from the ME effect, we conducted a similar experiment upon a Ni thin film that showed a stronger ME effect than NiFe. Based on microwave (MW) absorption arising from the SWR excitation as a function of the angle between the magnetization and the wave vector of the SAW, we confirmed that twofold symmetry appears in NiFe film, although the Ni film shows a mixed behavior with two- and fourfold symmetry. This inconsistency is attributed to whether the SWR is excited by the Barnett or ME fields. Moreover, we also found that the frequency dependence of the MW absorption arising from the SWR excitation was totally different

between the two cases. This result can be clearly explained by the analytical power-loss formula owing to the SWR excited by the Barnett and ME effects.

Let us consider a vorticity field excited by the R-SAW with vorticity along the z axis, injected into an $x-z$ semifinite ferromagnetic metal (FM). The distribution of the vorticity amplitude is given by [27]

$$\Omega^z = \frac{\omega^2 u_0}{c_t} e^{-k_t y} e^{i(kx-\omega t)}, \tag{2}$$

where ω is an angular frequency of R-SAW, u_0 is a deformation amplitude of R-SAW, c_t is the transverse velocity of a sound wave, and k is the longitudinal wave number. The transverse wave number k_t is given by $k_t = k\sqrt{1-\xi^2}$, where ξ is a constant given by $\xi \approx (0.875 + 1.12\nu)/(1+\nu)$ with Poisson ratio ν [18]. The vorticity in a FM leads to an alternating effective magnetic field along the vorticity. This is the Barnett field, which is given by

$$h_B^z = \frac{\Omega^z}{2\gamma} = \frac{\omega^2 u_0}{2c_t\gamma} e^{-k_t y} e^{i(kx-\omega t)}. \tag{3}$$

According to Eq. (3), the Barnett field is always parallel to Ω. In the case of R-SAW, Ω lies in plane, perpendicular to the propagation direction. The magnetic torque on magnetization at an angle ϕ from the propagation direction of R-SAW is, therefore, given by $h_B^z \cos\phi$. Consequently, the angular dependence of the SWR amplitude shows twofold symmetry and becomes maximal at $\phi = n\pi$. Moreover, the SWR amplitudes between the positive and negative magnetic fields are expected to be identical (i.e., reciprocal SWR). Note that the Barnett field is proportional to the square of the R-SAW frequency; thus, an increase of R-SAW frequency is critical for enhancement of the Barnett field in FM-thin films.

In addition to the Barnett effect, another dynamic field owing to the ME coupling is simultaneously generated when the R-SAW propagates through the FM. The change in free enthalpy caused by the ME effect is generally given by [28]

$$\begin{aligned} G^d = {} & b_1[\varepsilon_{xx}m_x^2 + \varepsilon_{yy}m_y^2 + \varepsilon_{zz}m_z^2] \\ & + 2b_2[\varepsilon_{xy}m_x m_y + \varepsilon_{xz}m_x m_z + \varepsilon_{yz}m_y m_z], \end{aligned} \tag{4}$$

where m_x, m_y, and m_z are the components of the unit vector of local magnetization $\boldsymbol{m} = \boldsymbol{M}/M$, and b_1 and b_2 are the ME-coupling constants. While Ni shows a strong ME effect as $b_1 = b_2 = 9.5\ \mathrm{MJ\,m^{-3}}$ [29], the $Ni_{19}Fe_{81}$ alloy hardly induces a ME effect as $b_1 = b_2 \sim 0\ \mathrm{MJ\,m^{-3}}$ at room temperature (polycrystalline film is assumed) [30]. $\varepsilon_{ij} = [(\partial u_i/\partial x_j) + (\partial u_j/\partial x_i)]/2$, with $i, j \in \{x, y, z\}$, are the strain-tensor components. A R-SAW contains the strain components ε_{xx}, ε_{xy}, and ε_{yy} [31]. The effective dynamic field due to the ME effect is given by $\boldsymbol{h}_{\mathrm{ME}} = -(\mu_0 M)^{-1}\partial_{\boldsymbol{m}} G^d|_{\boldsymbol{m}=\boldsymbol{m}_0}$, where $\boldsymbol{m}_0$ is the equilibrium direction of magnetization. When $\boldsymbol{M}$ lies in the film plane, the effective dynamic field consists of in- and out-of-plane components [22],

$$\boldsymbol{h}_{\mathrm{ME}}^{\mathrm{IP}} = \frac{2b_1}{\mu_0 M_s}\varepsilon_{xx}\sin\phi\cos\phi(\boldsymbol{m}_0 \times \boldsymbol{e}_y) \tag{5}$$

and

$$\boldsymbol{h}_{\mathrm{ME}}^{\mathrm{OOP}} = \frac{2b_2}{\mu_0 M_s}\varepsilon_{xy}\cos\phi\boldsymbol{e}_y, \tag{6}$$

respectively, where $\boldsymbol{e}_y$ is the unit vector along the y axis. The in-plane component $h_{\mathrm{ME}}^{\mathrm{IP}}$ is proportional to the longitudinal strain ε_{xx}, as depicted in Fig. 1(b), and shows fourfold in-plane symmetry, becoming maximal at $\phi = (1/2 + n)\cdot\pi/2$ [21]. On the other hand, the out-of-plane component $h_{\mathrm{ME}}^{\mathrm{OOP}}$ is proportional to the transverse strain ε_{xy}, as shown in Fig. 1(c), and shows twofold in-plane symmetry becoming maximal at $\phi = n\pi$ [25]. When both ε_{xx} and ε_{xy} coexist, the SWR intensities owing to these ME fields show different values between the positive and negative fields, i.e., nonreciprocal SWR [25,26]. The strain-tensor components generally depend upon frequency; for example, the ε_{xx} component in R-SAW is proportional to the R-SAW frequency because ε_{xx} is given by ku_0. The out-of-plane ME field is also roughly proportional to the frequency.

When a static magnetic field is applied in the FM film plane, a spin wave is excited due to the torque on magnetization given by the Barnett and/or ME fields, as shown in Figs. 1(a)–1(c). If the static field is applied parallel to the R-SAW-propagation direction, a magnetostatic backward-volume wave (MSBVW) is excited. The MW absorption in NiFe or Ni film, i.e., the R-SAW attenuation, can be measured using a vector network analyzer [16]. Figure 1(d) shows an experimental setup for observing SWR in a FM film. Two interdigital transducers (IDTs) consisting of 30-nm-thick Au were fabricated on a $LiNbO_3$ piezoelectric substrate. A MW with an amplitude of -5 dBm was transmitted from the left IDT (IDT1) and detected by the right IDT (IDT2). We used a 128° Y-cut $LiNbO_3$ substrate whose R-SAW-dispersion relation is given by $\omega = \xi c_t k$ [18]. The R-SAW is excited by a periodic electric field from the IDT. The wavelength of the excited R-SAW is consistent with the period of the IDT fingers. Consequently, we can vary the excitation frequency of the R-SAW by changing the structural period of the IDT. In our experiment, the R-SAW wavelength was varied from 1.8 to 3.0 μm at intervals of 0.2 μm, and consequent R-SAW excitation frequencies ranged from 1.3 to 2.1 GHz. A 400×400-μm^2 rectangle consisting of NiFe (20 nm) or

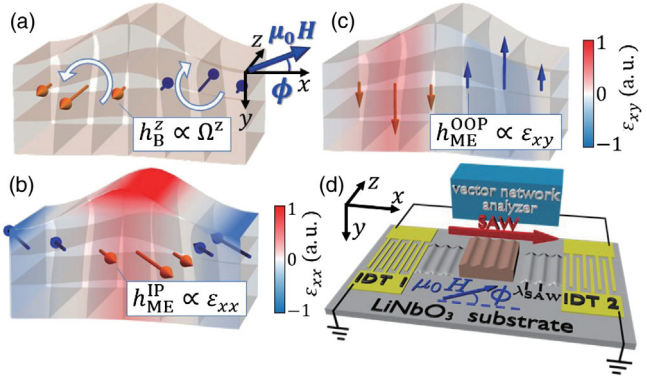

FIG. 1. (a)–(c) Schematic illustrations of effective dynamic fields originating from a R-SAW in a ferromagnetic thin film. The R-SAW propagates in the x direction and decays in the y (depth) direction. (a) A vorticity Ω^z yields a Barnett field along the z axis given by Eq. (3). (b),(c) A longitudinal strain ε_{xx} leads to a ME field $h_{\mathrm{ME}}^{\mathrm{IP}}$ in the plane, while a transverse strain ε_{xy} leads to a ME field $h_{\mathrm{ME}}^{\mathrm{OOP}}$ out of the plane, given by Eqs. (5) and (6), respectively. The color codes show the real parts of (b) ε_{xx} and (c) ε_{xy}. (d) Measurement setup for observing a SWR excited by effective dynamic fields. A R-SAW propagates between a pair of interdigital transducers on a $LiNbO_3$ piezoelectric substrate. A static field was applied in the plane at an angle of ϕ from the wave vector of the R-SAW. The R-SAW attenuation owing to SWR excitation can be measured from the S_{21} signal using a vector network analyzer.

Ni (20 nm) was deposited between IDTs. A static magnetic field ranging from −20 to 20 mT was applied in the FM film plane at an angle ϕ from the propagation direction of the R-SAW, as depicted in Fig. 1(d). We conducted a frequency-domain evaluation of the R-SAW amplitude at a given magnetic field by measuring the S_{21} parameter using a vector network analyzer.

It is noted that an electromagnetic excitation of spin waves was separated by time gating the measured S_{21} parameter as previously reported [16]. All measurements were conducted at room temperature.

Figure 2(a) shows a color plot of MW absorption as functions of frequency and magnetic field measured for a NiFe film. The static field was applied parallel to the propagation direction of the R-SAW ($\phi = 0$) and the structural period of the IDT was set to 2.4 μm. To avoid the influence of scattering in the amplitude of u_0 among the samples, we used the reduced MW absorption $\Delta P^{\mathrm{norm}}(f, H)$, defined as [16]

$$\Delta P^{\mathrm{norm}}(f, H) = \frac{|\boldsymbol{P}_{21}(f, H) - \boldsymbol{P}_{21}(f, H_{\mathrm{ref}})|}{P_{21}(f_{\mathrm{res}}, H_{\mathrm{ref}})}. \quad (7)$$

Here, $\boldsymbol{P}_{21}(f, H)$ is the complex power of the transmitted MW calculated from S_{21} at a given frequency f and magnetic field H. The reference magnetic field $\mu_0 H_{\mathrm{ref}} = -20$ mT is sufficient to saturate the magnetization of NiFe or Ni; thus, the field-independent signals can be removed by subtracting $\boldsymbol{P}_{21}(f, H_{\mathrm{ref}})$ from $\boldsymbol{P}_{21}(f, H)$. The transmitted MW intensity at the reference magnetic field is shown in Fig. 2(b). $P_{21}(f_{\mathrm{res}}, H_{\mathrm{ref}})$ in Eq. (7) corresponds to the peak magnitude of the complex power P_{21} at the R-SAW excitation frequency $f_{\mathrm{res}} = 1.615$ GHz. The magnitude of reduced MW absorption is independent of the R-SAW amplitude u_0, because both the R-SAW excitation power $P_{21}(f_{\mathrm{res}}, H_{\mathrm{ref}})$ and the MW absorption via Barnett and ME fields $|\boldsymbol{P}_{21}(f, H) - \boldsymbol{P}_{21}(f, H_{\mathrm{ref}})|$ are proportional to u_0^2 [16]. As shown in Figs. 2(a) and 2(b), large-MW absorption was observed at the frequency at which R-SAW was strongly excited. The MSBVW-dispersion relation at $\mu_0 M_s = 0.98$ T for the saturation magnetization of NiFe is indicated by the magenta guidelines in Fig. 2(a) (see Supplemental Material [32]). As shown in the enlargement of Fig. 2(a), strong MW absorption was observed at magnetic fields for which the excitation frequency of MSBVW matches the eigenfrequency of the R-SAW. Moreover, the SWR amplitude is similar between the positive and negative static fields, i.e., the excited SWR is reciprocal. These results suggest successful excitation of MSBVW via Barnett effect in NiFe. Similarly, the MW absorption and transmission measured for Ni using R-SAW with a wavelength of 2.4 μm for $\phi = \pi/4$ are shown in Figs. 2(c) and 2(d), respectively [32]. The magenta guidelines in Fig. 2(c) indicate the dispersion relations of the spin wave in Ni for $\phi = \pi/4$. Here, the SWR amplitude differs between the positive and negative static fields (see Supplemental Material [32]). Such nonreciprocity is attributable to the superposition effect of in- and out-of-plane dynamic ME fields [25].

A more explicit difference between the Barnett and ME effects is demonstrated by examining the ϕ dependence of the resonant fields and the SWR amplitude in NiFe and Ni. Figures 3(a) and 3(b) represent the SWR amplitude as functions of the static field and ϕ in NiFe and Ni,

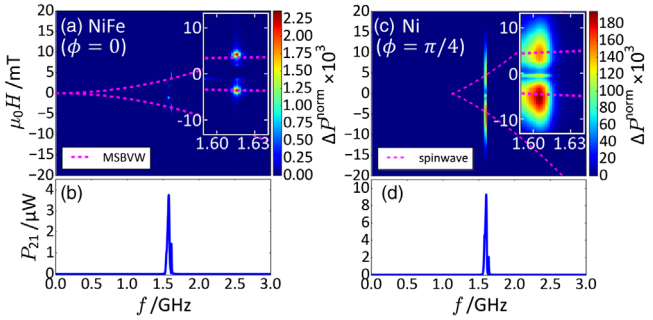

FIG. 2. (a) A color plot of MW absorption ΔP^{norm} as functions of frequency and static field, and (b) the frequency dependence of the MW transmission measured for NiFe film at $\phi = 0$. (c) The MW absorption and (d) transmission measured for Ni film at $\phi = \pi/4$. The period of the IDT finger was fixed at 2.4 μm. Magenta guidelines in (a) and (c) show the MSBVW-dispersion relations for NiFe and Ni films, respectively [32].

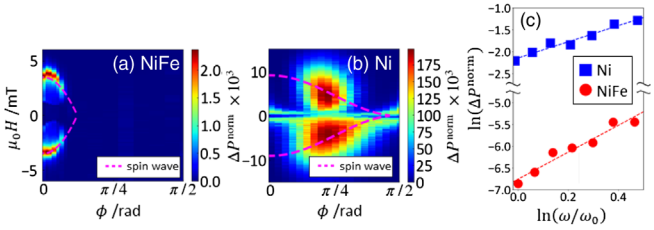

FIG. 3. The angular dependence of MW absorption in (a) NiFe and (b) Ni films. (c) R-SAW-frequency dependence of the MW absorption in NiFe ($\phi = 0$) and Ni ($\phi = \pi/4$). Magenta guidelines in (a) and (b) are the dispersion relations of the spin wave for NiFe and Ni films, respectively [32]. Broken lines in (c) show the results of best fit with Eq. (12).

respectively. The MW frequency was fixed at the R-SAW excitation frequency, at which the SWR amplitude became maximal in Figs. 2(a) and 2(c). Magenta guidelines in Figs. 3(a) and 3(b) are the dispersion relations of the spin wave [32]. While the resonant fields agreed well with the dispersion relations in both NiFe and Ni, the angular dependence of the SWR amplitude was quite different; the SWR amplitude in NiFe became maximal at $\phi = 0$ and gradually decreased with increasing ϕ. By contrast, the SWR amplitude in Ni gradually increased with ϕ and became maximal at $\phi = (2/9)\pi$, followed by decrease with increasing ϕ. The former is consistent with the angular dependence of the Barnett field that is maximized at $\phi = 0$, and the latter can be explained by considering the mixed-ME fields that are maximized at an angle slightly less than $\pi/4$, which is attributable to the coexistence of majority ε_{xx} and minority ε_{xy} in the R-SAW, as previously reported [21,22]. The explicit difference in the angular dependence of MW absorption is definitive evidence that the Barnett and ME fields excite SWR in the NiFe and Ni films, respectively.

Second, we compared the frequency dependences of MW absorption in NiFe and Ni, as shown in Fig. 3(c) in the form of a double-logarithmic plot. In order to quantitatively evaluate the Barnett and ME fields, we calculated the power loss owing to the magnetic torques from these fields. The magnetization dynamics are generally described by the Landau-Lifshitz-Gilbert equation

$$\frac{\partial \boldsymbol{M}}{\partial t} = -\gamma[\boldsymbol{M} \times \boldsymbol{H}_{\rm eff}] + \frac{\alpha}{M}\left[\boldsymbol{M} \times \frac{\partial \boldsymbol{M}}{\partial t}\right], \tag{8}$$

where $\boldsymbol{M}$ is the vector of local magnetization and α is the Gilbert damping coefficient. $\boldsymbol{H}_{\rm eff}$ is the effective field given by

$$\boldsymbol{H}_{\rm eff} = \boldsymbol{H} - \overleftrightarrow{N}\boldsymbol{M} + \boldsymbol{h}_B + \boldsymbol{h}_{\rm ME}^{\rm IP} + \boldsymbol{h}_{\rm ME}^{\rm OOP}, \tag{9}$$

which consists of the static magnetic field, demagnetizing field, Barnett field, and in- and out-of-plane components of the ME field. From the relation $P_{\rm SAW} = \omega M_{\rm el} W u_0^2$ [34], where $M_{\rm el} = 1.4 \times 10^{11}$ Jm^{-3} is a material constant for $LiNbO_3$ and $W = 355$ μm is the finger length of IDT, the reduced MW absorption is expressed as

$$\Delta P^{\rm norm} = \frac{1}{\omega M_{\rm el} W u_0^2} \frac{\mu_0 \omega}{2\pi} \int \boldsymbol{H}_{\rm eff} d\boldsymbol{M}. \tag{10}$$

For a small-precession limit, $\boldsymbol{M}$ can be approximated as $\boldsymbol{M} \approx (M_s, M_y e^{i\omega t}, M_z e^{i\omega t})$, where $|M_y|, |M_z| \ll M_s$. Finally, Eq. (10) is calculated as

$$\begin{aligned}\Delta P^{\rm norm} &= \Delta P_B^{\rm norm} + \Delta P_{\rm ME,OOP}^{\rm norm} + \Delta P_{\rm ME,IP}^{\rm norm} + \text{cross terms} \\ &\approx \frac{\gamma \mu_0 M_s}{2\alpha M_{\rm el} W \omega}\left[\left\{\left|\frac{h_B^z}{u_0}\right|^2 + \frac{\omega^2}{\omega_y^2}\left|\frac{h_{\rm ME}^{\rm OOP}}{u_0}\right|^2\right\} + \left|\frac{h_{\rm ME}^{\rm IP}}{u_0}\right|^2\right] \\ &\quad + \text{cross terms} \end{aligned} \tag{11}$$

$$\approx A_0\left(\frac{\omega}{\omega_0}\right)^3 + B_0\left(\frac{\omega}{\omega_0}\right)^1 + 2\sqrt{A_0 B_0}\left(\frac{\omega}{\omega_0}\right)^2, \tag{12}$$

where $\omega_y = \gamma M_s$. The formulas of A_0 and B_0 in Eq. (12) are shown in the Supplemental Material [32]. The first–fourth terms in Eq. (11) correspond to the contributions of the Barnett field, the in- and out-of-plane components of the ME field, and their products, respectively. Note that $\Delta P^{\rm norm}$ in Eq. (11) is independent of u_0 because both the Barnett and ME fields are proportional to u_0. The contributions of the out-of-plane ME fields are two powers of frequency higher than that of the in-plane ME field because of differences in relative orientation with respect to the demagnetizing field. By substituting Eqs. (3), (5), and (6) into Eq. (11), one obtains Eq. (12), which shows the frequency dependence of $\Delta P^{\rm norm}$ explicitly, where $\omega_0 = 2\pi \times 1.30$ GHz. The contributions of both the Barnett and out-of-plane ME fields are proportional to the third order of frequency, while the in-plane ME field leads to first-order variation with respect to frequency. From Fig. 3(c), we find that the values of the gradient of the double-logarithmic plot were 3.1 and 1.8 for the NiFe ($\phi = 0$) and Ni ($\phi = \pi/4$) films, respectively. Both the angular and frequency dependences of $\Delta P^{\rm norm}$ imply that the SWR in NiFe is excited by the Barnett field. From the SWR intensity at a frequency of 1.60 GHz, we can evaluate the R-SAW amplitude averaged along the film thickness and the subsequent Barnett field to be $u_0 = 6.3$ pm and $\mu_0 h_B^z = 1.2$ μT when a microwave with an amplitude of -5 dBm is applied to the IDT [35]. We can also conclude that the in- and out-of-plane ME fields excited the SWR in Ni because the gradient of the double-logarithmic plot was between 1 and 3. In fact, a nonreciprocity in SWR intensity between the positive and negative static fields [25] (which is expected when ε_{xx} and ε_{xy} coexist) appeared, as seen in Fig. 2(c).

Finally, we emphasize that the SWR in the NiFe monolayer is excited in the manner totally different from the previous method in the NiFe/Cu bilayer where the spin transfer torque (STT) produced by spin-current injection from an adjacent nonmagnetic Cu film is significant for the SWR excitation (see Supplemental Material [32]). It is expected that the SAW injection to the NiFe/Cu bilayer can also lead to the Barnett effect in addition to the STT-driven SWR. However, from the comparison in the amplitude of ΔP^{norm}, we confirm that the amplitude of the STT-driven SWR in the NiFe/Cu bilayer [16] is 60 times larger than the Barnett effect-driven SWR observed in the NiFe monolayer. The comparison suggests that the STT is much stronger than the torque caused by the Barnett effect. The SWR owing to the Barnett effect was, therefore, hidden in the NiFe/Cu bilayer. Unlike the previous study, we do not need an adjacent nonmagnetic layer for the SWR excitation because the STT owing to the spin current is not necessary. Moreover, we do not use the ME effect to excite the SWR. These features enhance a degree of freedom in material design in the spintronics devices in which soft magnetic materials with small magnetic anisotropy are widely utilized.

In summary, we demonstrated the gyromagnetic spin wave excitation in a NiFe thin film via the Barnett effect using the R-SAW. The MW absorption owing to SWR excitation by the Barnett and ME fields can be distinguished from the difference in the variation with respect to the MW frequency and the angle of field application. By using the gigahertz SAW, we succeeded in producing a Barnett field in metallic ferromagnets with a large gyromagnetic ratio and weak magnetoelastic coupling, which is hard to realize by a rigid rotation with kilohertz frequency, as seen in centrifuge experiments [9–14]. Our technique paves the way to utilize the Barnett field to excite magnons in solid-state spintronic devices.

This work was partially supported by JST CREST Grant No. JPMJCR19J4, Japan, JSPS KAKENHI Grant No. JP18H03867, and M. M. was partially supported by the Priority Program of Chinese Academy of Sciences Grant No. XDB28000000.

[1] S. J. Barnett, Phys. Rev. **6**, 239 (1915).
[2] S. J. Barnett, Rev. Mod. Phys. **7**, 129 (1935).
[3] A. Einstein and W. J. De Haas, Proc. KNAW **18**, 696 (1915), https://www.dwc.knaw.nl/DL/publication/PU00012546.pdf.
[4] C. G. de Oliverira and J. Tiomno, Nuovo Cimento **24**, 672 (1962).
[5] B. Mashhoon, Phys. Rev. Lett. **61**, 2639 (1988).
[6] J. Anandan, Phys. Rev. Lett. **68**, 3809 (1992).
[7] B. Mashhoon, Phys. Rev. Lett. **68**, 3812 (1992).
[8] F. W. Hehl and W.-T. Ni, Phys. Rev. D **42**, 2045 (1990).
[9] H. Chudo, M. Ono, K. Harii, M. Matsuo, J. Ieda, R. Haruki, S. Okayasu, S. Maekawa, H. Yasuoka, and E. Saitoh, Appl. Phys. Express **7**, 063004 (2014).
[10] H. Chudo, K. Harii, M. Matsuo, J. Ieda, M. Ono, S. Maekawa, and E. Saitoh, J. Phys. Soc. Jpn. **84**, 043601 (2015).
[11] K. Harii, H. Chudo, M. Ono, M. Matsuo, J. Ieda, R. Haruki, S. Okayasu, S. Maekawa, and E. Saitoh, Jpn. J. Appl. Phys. **54**, 050302 (2015).
[12] M. Ono, H. Chudo, K. Harii, S. Okayasu, M. Matsuo, J. Ieda, R. Takahashi, S. Maekawa, and E. Saitoh, Phys. Rev. B **92**, 174424 (2015).
[13] M. Imai, Y. Ogata, H. Chudo, M. Ono, K. Harii, M. Matsuo, Y. Ohnuma, S. Maekawa, and E. Saitoh, Appl. Phys. Lett. **113**, 052402 (2018).
[14] M. Imai, H. Chudo, M. Ono, K. Harii, M. Matsuo, Y. Ohnuma, S. Maekawa, and E. Saitoh, Appl. Phys. Lett. **114**, 162402 (2019).
[15] R. Takahashi, M. Matsuo, M. Ono, K. Harii, H. Chudo, S. Okayasu, J. Ieda, S. Takahashi, S. Maekawa, and E. Saitoh, Nat. Phys. **12**, 52 (2016).
[16] D. Kobayashi, T. Yoshikawa, M. Matsuo, R. Iguchi, S. Maekawa, E. Saitoh, and Y. Nozaki, Phys. Rev. Lett. **119**, 077202 (2017).
[17] G. Okano, M. Matsuo, Y. Ohnuma, S. Maekawa, and Y. Nozaki, Phys. Rev. Lett. **122**, 217701 (2019).
[18] M. Matsuo, J. Ieda, K. Harii, E. Saitoh, and S. Maekawa, Phys. Rev. B **87**, 180402(R) (2013).
[19] J. Ieda, M. Matsuo, and S. Maekawa, Solid State Commun. **198**, 52 (2014).
[20] M. Matsuo, Y. Ohnuma, and S. Maekawa, Phys. Rev. B **96**, 020401(R) (2017).
[21] M. Weiler, L. Dreher, C. Heeg, H. Huebl, R. Gross, M. S. Brandt, and S. T. B. Goennenwein, Phys. Rev. Lett. **106**, 117601 (2011).
[22] L. Dreher, M. Weiler, M. Pernpeintner, H. Huebl, R. Gross, M. S. Brandt, and S. T. B. Goennenwein, Phys. Rev. B **86**, 134415 (2012).
[23] X. Li, D. Labanowski, S. Salahuddin, and C. S. Lynch, J. Appl. Phys. **122**, 043904 (2017).
[24] D. Labanowski, A. Jung, and S. Salahuddin, Appl. Phys. Lett. **108**, 022905 (2016).
[25] R. Sasaki, Y. Nii, Y. Iguchi, and Y. Onose, Phys. Rev. B **95**, 020407(R) (2017).
[26] M. Xu, J. Puebla, F. Auvray, B. Rana, K. Kondou, and Y. Otani, Phys. Rev. B **97**, 180301(R) (2018).
[27] L. D. Landau and E. M. Lifshitz, *Theory of Elasticity* (Pergamon, New York, 1959).
[28] S. Chikazumi, *Physics of Ferromagnetism*, 2nd ed. (Oxford University Press, Oxford, 1997).
[29] E. Klokholm and J. Aboaf, J. Appl. Phys. **53**, 2661 (1982).
[30] I. W. Wolf and T. S. Crowther, J. Appl. Phys. **34**, 1205 (1963).
[31] A. N. Clealand, *Foundations of Nanomechanics* (Springer, Berlin, 2003).
[32] See Supplemental Material at http://link.aps.org/supplemental/10.1103/PhysRevLett.124.217205 for dispersion relation of the spin wave excited in ferromagnetic thin films, microwave absorption ΔP^{norm} at $\phi = 0$ and $\pi/4$ as functions of frequency and static field for NiFe and Ni films, nonreciprocal spin wave resonance due to the magnetoelastic effect in a Ni film, threshold angle of static field for spin wave resonance excitation, and comparison of

the role of gyromagnetic effect in the spin wave resonance between NiFe monolayer and NiFe/Cu bilayer films, which includes Ref. [16,21,25,26,33].

[33] K. Y. Guslienko, R. W. Chantrell, and A. N. Slavin, Phys. Rev. B **68**, 024422 (2003).

[34] W. Robbins, IEEE Trans. Sonics Ultrason. **24**, 339 (1977).

[35] We can assume that the value of u_0 is homogeneous along the thickness direction because the NiFe film is much thinner than the decay length of the SAW.